their closed-shell electronic configurations and more extensive metal–metal bonding. The clusters represented contain the weak-field, anionic terminal ligands L = RS^-, RO^-, and halide and span the nuclearities 2–8.

It is immediately evident that prismane and basket clusters are topological isomers and that the Fe_2S_2 rhomb (albeit of varying dimensions) is the building block of all known Fe–S clusters. Indeed, the basket cluster is the only one not built up entirely by the connection of rhombs at a common point or their fusion at edges. We have previously documented[1-3] the conversion and/or interconversion of all clusters, except $[Fe_6S_9(SR)_2]^{4-}$, $[Fe_6S_8(PEt)_6]^{2+,+}$, and $[Fe_8S_6I_8]^{3-}$, in reactions that afford only one cluster product, often with known stoichiometry. One cluster not listed in Table IV is the trinuclear core entity $[Fe_3S_4]^{+,0}$, found in a number of proteins but not yet prepared outside a protein environment. Crystallographic results for aconitase[35] and a recent redetermination of the structure of *Azotobacter vinelandii* ferredoxin II[36] indicate a triangular Fe_3 arrangement and the voided-cubane structure $Fe_3(\mu_3\text{-}S)(\mu_2\text{-}S)_3$. These units can be reconstituted to the corresponding Fe_4S_4 cubanes,[37] providing another example of cluster conversion.

Summary. The following are the principal findings and conclusions from this investigation.

1. The iron–sulfur–thiolate basket clusters $Fe_6S_6(PEt_3)_4(SR)_2$ (R = arene) may be prepared in 65–70% purified yield by cluster self-assembly $(Fe(PEt_3)_2(SR)_2 + (Me_3Si)_2S)$ or cluster expansion $(Fe(PEt_3)_2(SPh)_2 + [Fe_4S_4(SPh)_4]^{2-})$ in THF solution. The latter process and ligand substitution (vide infra) are the preferred methods of synthesis.

2. The $[Fe_6(\mu_4\text{-}S)(\mu_3\text{-}S)_4(\mu_2\text{-}S)]^{2+}$ core of $Fe_6S_6(PEt_3)_4(S\text{-}p\text{-}C_6H_4Br)_2$ is essentially congruent with that of $Fe_6S_6(PBu_3)_4Cl_2$ and consists of six nonplanar Fe_2S_2 rhombs fused to form a basket with the bridge unit Fe–S–Fe acting as the handle.

3. Basket stereochemistry is retained in solution and is maintained in thiolate–chloride substitution reactions.

4. The baskets $Fe_6S_6(PEt_3)_4L_2$ (L = RS^-, halide) are the newest type of Fe–S cluster. They are topological isomers of prismane clusters and form part of a set of Fe–S clusters of nuclearities 2, 3, 4, 6, and 7 whose core structures may be converted or interconverted under mild conditions.

It is apparent that neither the coherence nor complexity of Fe–S cluster chemistry has been exhausted. For example, in this laboratory[26] we have characterized a basket cluster, $[Fe_6S_6(PEt_3)_6]^+$, lacking anionic terminal ligands, and found it to be a synthetic precursor to at least one other cluster topology. Additionally, we have identified a cluster of core composition $Fe_{18}S_{30}$ of an entirely different overall structure than has been encountered previously.[38] These clusters, together with the electronic properties of basket clusters, will be the subjects of subsequent reports.

Acknowledgment. This research was supported by National Institutes of Health Grant GM 28856. NMR and X-ray diffraction equipment was obtained through National Science Foundation Grants CHE 80-00670 and CHE 80-08891. We thank Derk Wierda and Dr. Simon Bott for helpful crystallographic discussions.

Supplementary Material Available: For $Fe_6S_6(PEt_3)_4(S\text{-}p\text{-}C_6H_4Br)_2$, a stereoview and tables of crystal data, intensity collection, and refinement parameters, atom thermal parameters, interatomic distances and angles, and calculated hydrogen atom positions (11 pages); a table of calculated and observed structure factors (51 pages). Ordering information is given on any current masthead page.

(35) Robbins, A. H.; Stout, C. D. *J. Biol. Chem.* **1985**, *260*, 2328.
(36) (a) Stout, G. H.; Turley, S.; Sieker, L. C.; Jensen, L. H. *Proc. Natl. Acad. Sci U.S.A.* **1988**, *85*, 1020. (b) Stout, C. D. *J. Biol. Chem.* **1988**, *263*, 9256.
(37) (a) Kent, T. A.; Dreyer, J.-L.; Kennedy, M. C.; Huynh, B.-H.; Emptage, M. H.; Beinert, H.; Münck, E. *Proc. Natl. Acad. Sci U.S.A.* **1982**, *79*, 1096. (b) Kennedy, M. C.; Emptage, M. H.; Dreyer, J.-L.; Beinert, H. *J. Biol. Chem.* **1983**, *258*, 11098. (c) Moura, J. J. G.; Moura, I.; Kent, T. A.; Lipscomb, J. D.; Huynh, B.-H.; LeGall, J.; Xavier, A. V.; Münck, E. *J. Biol. Chem.* **1982**, *257*, 6259.
(38) You, J.-F.; Snyder, B. S.; Holm, R. H. *J. Am. Chem. Soc.* **1988**, *110*, 6589.

Contribution from the Department of Chemistry, Colorado State University, Fort Collins, Colorado 80523

A Triply Bridged Dinuclear Tris(bipyridine)iron(II) Complex: Synthesis and Electrochemical and Structural Studies

Barbara R. Serr, Kevin A. Andersen, C. Michael Elliott,* and Oren P. Anderson

Received April 14, 1988

A triply bridged dinuclear iron complex consisting of three bridging bis[4-(2,2′-bipyridinyl)]ethane ligands linking the two Fe(II) centers has been synthesized. An X-ray crystallographic study has confirmed the dinuclear structure. Cyclic voltammetry, differential-pulse voltammetry, and Osteryoung square-wave voltammetry studies have been conducted on the dinuclear iron complex and on the corresponding $Fe^{II}(4,4'\text{-}Me_2bpy)_3$ mononuclear complex. The electrochemistry of the dinuclear complex demonstrates that there exists significant interaction between the two iron centers. Given that the ligand bridges consist of saturated hydrocarbon linkages, through-bond interactions are not important, and thus the observed effects are purely through-space and electrostatic in nature.

Introduction

Symmetric dinuclear metal complexes have long been of interest with regard to studying phenomena associated with mixed-valence oxidation states.[1] When two redox active metal centers are linked via a bridging ligand or by a direct bond, the redox potential of one of the two centers can be influenced by the oxidation state of the other. When the bridging moiety is a single atom, a bond, or a molecule containing conjugated unsaturation, the possibility exists for charge delocalization over the two centers. In one extreme case, the second site becomes thermodynamically harder to oxidize or reduce than the first, producing, for example, a splitting of the cyclic voltammetric waves into two separated one-electron processes. In the other extreme case, the second electron-transfer process becomes thermodynamically easier than the first, resulting in a formal two-electron process, characterized by a single cyclic voltammetric wave having a peak separation of 30 mV. On the other hand, if the valence is localized and the two sites are far apart, the cyclic voltammogram is indistin-

(1) (a) Richardson, D. E.; Taube, H. *J. Am. Chem. Soc.* **1983**, *105*, 40. (b) Sutton, J. E.; Taube, H. *Inorg. Chem.* **1981**, *20*, 3125.

0020-1669/88/1327-4499$01.50/0

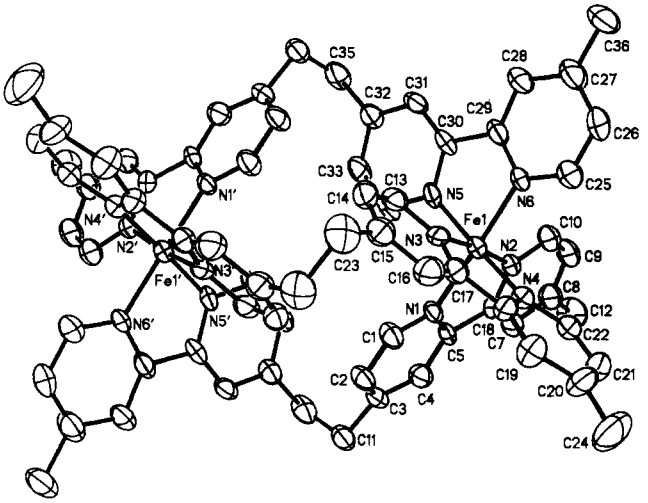

Figure 1. Structure of the cationic unit of I $[Fe_2(Mebpy\text{-}Mebpy)_3]^{4+}$.

guishable from that obtained from a simple one-electron couple.[2] In this latter case, the electrons are distributed statistically between all redox sites: for example, if exactly one electron per dinuclear unit were to be added, 25% of the molecules would be unreduced, 25% would be doubly reduced, and 50% would be singly reduced (i.e. "mixed-valence"). If, however, the redox sites are very close together, site–site interaction is possible even when the charges are completely localized. This type of interaction is electrostatic in origin and occurs through space rather than through bonds. However, few unambiguous examples of pure electrostatic interactions have been demonstrated.[1] Since a minimum of one CH_2–CH_2 unit (or some equivalent saturated unit) must be present in the bridge to insure that no through-bond interaction occurs, centers in such complexes are typically fairly far apart. Since the electrostatic potential decreases as $1/r$, under typical electrochemical conditions (relatively high dielectric medium), the sites are usually too far apart to reflect any interaction.

Herein, we report the synthesis and electrochemical characterization of a symmetric Fe(II) dinuclear tris(bipyridine) complex that is triply linked by three saturated two-carbon bridges (Figure 1). Because of the triply bridged nature of the complex, the two metal centers are rigidly held at a distance of 7.646(3) Å. This separation is considerably shorter than for analogous singly bridged complexes which are free to rotate around the alkane bridge and thus maximize the charge separation.[3] For example, on the basis of molecular models, the bis(pyridinyl)ethane-bridged Ru complexes studied by Meyer et al.[3] can attain a metal–metal separation of ~14 Å. Finally, both the formation of I and its electrochemistry can be explained semiquantitatively on the basis of relatively strong, through-space electrostatic interactions.

Experimental Section

Measurements. All electrochemical measurements were carried out in O_2 free, nitrogen-purged acetonitrile solutions with 0.1 M tetra-*n*-butylammonium hexafluorophosphate [(TBA)PF_6] as supporting electrolyte. A conventional three-electrode cell was used with a 0.71 mm^2 glassy-carbon working electrode, a platinum-wire loop auxiliary electrode, and a saturated calomel electrode (SCE) as reference.

Cyclic volammetry was performed by using a PAR Model 173 potentiostat. Differential-pulse voltammetry and Osteryoung square-wave voltammetry were performed with a BAS-100 Electrochemical Analyzer.

Materials. All reagents and solvents were purchased commercially and used without further purification except for the following. (TBA)PF_6 was prepared as previously reported,[6] recrystallized three times from hot ethanol and dried under vacuum. 4,4′-Dimethyl-2,2′-bipyridine (Me_2bpy) was recrystallized from ethyl acetate before use. 1,2-Bis[4-(4′-methyl-2,2′-bipyridinyl)]ethane (Mebpy-Mebpy) was prepared as previously described.[7]

The eluent for thin-layer chromatography (TLC) was a 50% acetonitrile, 40% water, and 10% saturated aqueous KNO_3 (by volume) solution.

Preparation of $Fe_2(Mebpy\text{-}Mebpy)_3$ (I). In a typical preparation, 78 mg (0.071 mmol) of Mebpy-Mebpy was dissolved in approximately 10 mL of acetone. To this solution was added a solution of 22 mg (0.047 mmol) of $FeSO_4$ in about 40 mL of water. An immediate color change from colorless to red marked the complex formation. The resulting solution was heated and stirred to allow evaporation of the acetone, with water added as needed to maintain the volume. After no detectable odor of acetone remained (~30 min), the solution was removed from heat and allowed to cool. A 10-fold excess of ammonium hexafluorophosphate (NH_4PF_6) was added to precipitate the product. The precipitate was collected and dried under vacuum at 75 °C for 12 h. TLC on silica revealed the presence of a single product.

The triflate salt of I was prepared as described above, except a 50-fold excess of HO_3SCF_3 was added to precipitate the product. Single crystals of the triflate salt of suitable size and quality for X-ray diffraction studies were grown by vapor diffusion of pentane into a solution of the triflate salt of I in acetone.

Preparation of $[Fe(Me_2bpy)_3](PF_6)_2$ (II). In a typical preparation, 83 mg (0.45 mmol) of Me_2bpy was dissolved in approximately 60 mL of hot acetone. To this solution was added a solution of 41 mg (0.15 mmol) of $FeSO_4$ in about 40 mL of water. Again, an immediate color change from colorless to red marked the formation of the complex. The product was obtained from the solution in the same manner as described for I. TLC again showed only one detectable product.

Preparation of $[(Me_2bpy)_2Ru(Mebpy\text{-}Mebpy)Ru(Me_2bpy)_2](PF_6)_4$ (III). In a typical preparation, 25 mg of $Ru(bpy)_2Cl_2$ (5.2×10^{-5} mol) and 9.2 mg of Mebpy-Mebpy (2.5×10^{-5} mol) were dispersed in ~20 mL of ethylene glycol. The solution was heated to ~140 °C for 15 min whereupon all solids had dissolved and the solution turned yellow-orange. After the solution was cooled, the volume was brought to 50 mL by addition of H_2O. The complex was precipitated by the addition of NH_4PF_6 solution, filtered, washed with several portions of water, and dried under vacuum.

Crystallographic Study. A crystal of the triflate salt of compound I was centered on a Nicolet R3m diffractometer. Centering of 25 reflections ($2\theta_{av} = 18.37°$) allowed least squares calculation[4] of the cell constants given in Table I. Other details regarding the experiment and the computations are also listed in Table I.

The stability of the crystal in the X-ray beam was monitored during data collection by measurement of the intensities of three control reflections (600, 020, 004) every 97 reflections. Anisotropic decay of these intensities was noted during data collection, with the intensities of the 020 and 004 reflections dropping by approximately 30% and 45%, respectively. The ω-scans of the 00*l* reflection showed that a crack in the crystal had developed. Lorentz and polarization corrections were applied to the data, as well as a crude correction for this anisotropic intensity decay. No absorption correction was applied, due to the small absorption coefficient.

Systematic reflection conditions suggested either the space group $C2/c$

Table I. Crystallographic Data for I

chem formula	$[C_{72}H_{66}Fe_2N_{12}]^{4+}\cdot 4[CF_3SO_3]^-\cdot 2(CH_3)_2CO\cdot H_2O$
fw	1959.5
space group	$C2/c$ (No. 15)
a, Å	32.69 (1)
b, Å	14.573 (3)
c, Å	27.314 (6)
β, deg	133.72 (2)
V, Å^3	9404 (2)
T, °C	−63
Z	4
λ, Å	0.710 73 (Mo Kα)
μ, cm^{-1}	4.83
ρ_{calc}, g cm^{-3}	1.38
data/param ratio	9.2
R	0.119
R_w	0.129

(2) Flanagan, J. B.; Margel, S.; Bard, A. J.; Anson, F. C. *J. Am. Chem. Soc.* **1978**, *100*, 4248.
(3) Callahan, R. W.; Brown, G. M.; Meyer, T. J. *Inorg. Chem.* **1975**, *14*, 1443.
(4) Calculations for diffractometer operations were performed by using software supplied with the Nicolet R3m diffractometer. All structural calculations were performed with the SHELXTL program library written by Professor G. M. Sheldrick and supplied by Nicolet XRD Corp.
(5) *International Tables for X-ray Crystallography*; Kynoch: Birmingham, England, 1974; Vol. IV, pp 99, 149.
(6) Elliott, C. M.; Hershenhart, E.; Finke, R. G.; Smith, B. L. *J. Am. Chem. Soc.* **1981**, *103*, 5558.
(7) Elliott, C. M.; Freitag, R. A.; Blaney, D. D. *J. Am. Chem. Soc.* **1985**, *107*, 4647.

Table II. Atomic Coordinates ($\times 10^4$) and Isotropic Thermal Parameters ($Å^2 \times 10^3$)[a] for Compound I

atom	x	y	z	U_{iso}[b]
Fe1	1040 (1)	3244 (1)	2288 (1)	35 (1)*
N1	1275 (2)	2904 (4)	3152 (3)	31 (4)*
N2	1492 (2)	2157 (5)	2501 (3)	39 (4)*
N3	637 (2)	4357 (4)	2166 (3)	35 (4)*
N4	1674 (3)	4106 (5)	2802 (3)	41 (4)*
N5	363 (3)	2487 (4)	1719 (3)	37 (4)*
N6	788 (3)	3495 (4)	1407 (3)	39 (4)*
C1	1146 (3)	3348 (5)	3464 (4)	40 (5)*
C2	1306 (3)	3049 (5)	4042 (4)	39 (5)*
C3	1620 (3)	2251 (6)	4344 (3)	40 (5)*
C4	1784 (3)	1801 (5)	4051 (4)	41 (5)*
C5	1604 (3)	2145 (5)	3459 (3)	36 (4)*
C6	1741 (3)	1727 (5)	3090 (3)	37 (4)*
C7	2089 (3)	967 (6)	3326 (4)	46 (5)*
C8	2169 (4)	594 (6)	2929 (4)	52 (6)*
C9	1890 (4)	1012 (7)	2313 (4)	60 (7)*
C10	1568 (4)	1769 (7)	2122 (4)	54 (6)*
C11	1742 (3)	1827 (6)	4950 (4)	48 (5)*
C12	2553 (4)	−229 (7)	3167 (5)	71 (8)*
C13	80 (3)	4457 (5)	1789 (3)	40 (5)*
C14	−157 (3)	5261 (5)	1760 (4)	43 (5)*
C15	177 (3)	6007 (5)	2136 (4)	42 (5)*
C16	757 (3)	5915 (6)	2523 (4)	49 (6)*
C17	971 (3)	5099 (5)	2523 (4)	38 (5)*
C18	1571 (3)	4957 (6)	2907 (4)	43 (5)*
C19	1984 (4)	5616 (7)	3317 (4)	60 (7)*
C20	2544 (4)	5404 (8)	3624 (5)	68 (6)*
C21	2641 (4)	4543 (7)	3503 (4)	59 (6)*
C22	2224 (3)	3919 (7)	3118 (4)	50 (5)*
C23	−62 (4)	6855 (6)	2176 (5)	57 (7)*
C24	3001 (5)	6081 (10)	4092 (7)	99 (10)*
C25	1048 (4)	4044 (7)	1294 (4)	58 (6)*
C26	837 (4)	4214 (7)	665 (5)	64 (7)*
C27	315 (4)	3881 (7)	103 (4)	60 (7)*
C28	30 (4)	3315 (7)	209 (4)	56 (6)*
C29	286 (3)	3132 (5)	864 (4)	41 (5)*
C30	30 (3)	2553 (5)	1042 (4)	38 (5)*
C31	−490 (3)	2122 (5)	571 (4)	40 (5)*
C32	−687 (3)	1581 (5)	788 (4)	39 (5)*
C33	−333 (3)	1481 (5)	1490 (4)	41 (6)*
C34	165 (4)	1933 (5)	1923 (4)	41 (6)*
C35	−1269 (4)	1165 (6)	295 (4)	52 (6)*
C36	78 (5)	4079 (10)	−586 (5)	83 (8)*
S1	1996 (1)	5422 (2)	4754 (1)	76 (2)*
O1	1498 (3)	5396 (5)	4042 (3)	79 (5)*
O2	2023 (5)	4822 (7)	5157 (4)	120 (8)*
O3	2528 (4)	5438 (10)	4956 (6)	153 (9)*
Ct1	1918 (7)	6556 (11)	4978 (9)	135 (15)*
F1	2363 (5)	6725 (7)	5633 (6)	199 (12)*
F2	1876 (7)	7174 (7)	4647 (8)	236 (18)*
F3	1458 (5)	6615 (9)	4850 (8)	215 (16)*
S2a	1689 (2)	7137 (4)	1713 (3)	79 (4)*
S2b	1494 (4)	7864 (7)	1468 (4)	98 (6)*
O4a	1695 (14)	6271 (11)	1943 (19)	228 (53)*
O5a	1679 (10)	7501 (16)	1179 (10)	180 (26)*
O6a	2265 (6)	7486 (12)	2299 (9)	121 (14)*
O4b	983 (16)	8018 (24)	1051 (19)	165 (12)
O5b	1642 (16)	8877 (27)	1716 (19)	147 (14)
O6b	1520 (7)	7351 (12)	1185 (9)	70 (4)
C2a	1322 (9)	7830 (14)	1821 (12)	106 (19)*
C2b	1655 (17)	7095 (29)	2128 (20)	113 (12)
F4a	1556 (7)	7679 (10)	2480 (7)	124 (15)*
F5a	1411 (7)	8727 (9)	1786 (10)	135 (18)*
F6a	768 (5)	7710 (11)	1311 (9)	146 (14)*
F4b	1355 (10)	7363 (16)	2239 (11)	132 (7)
F5b	2226 (14)	7343 (22)	2625 (17)	190 (12)
F6b	1490 (9)	6257 (15)	1765 (11)	125 (7)
Ow1	1157 (4)	5925 (7)	74 (6)	120 (11)*
Ca1	976 (13)	9378 (16)	2998 (21)	272 (45)*
Ca2	1293 (12)	8810 (18)	3415 (17)	308 (33)*
Ca3	740 (12)	9378 (18)	2222 (12)	210 (30)*
Oa1	875 (9)	10116 (16)	3037 (11)	263 (28)*

[a] Estimated standard deviations in the least significant digits are given in parentheses. [b] For values marked with asterisks, the equivalent isotropic U is defined as one-third of the trace of the U_{ij} tensor.

(no. 15) or *Cc* (no. 9); with $Z = 4$ in $C2/c$, the dinuclear cation must possess either 2 or $\bar{1}$ symmetry. The position of a single heavy atom was obtained from the Patterson map; that solution confirmed that the cation possessed the crystallographically required 2-fold rotation symmetry. The placement of the iron atom allowed the remaining non-hydrogen atoms of the symmetry-unique half of the dinuclear cation to be readily located in difference electron density maps. Two counterions ($CF_3SO_3^-$) were also located in general positions within the asymmetric unit. Unfortunately, one of these triflate groups was disordered. The final model used to describe the disordered triflate group involved two discrete orientations of the anion. The site occupancy factor for these fractional anions was refined; convergence indicated that a 60:40 ratio of the two orientations was appropriate. In addition, an occluded acetone molecule was located and included in the refinement.

Table III. Selected Bond Lengths (Å) and Angles (deg) for Compound I

(a) Bond Lengths

Fe1–Fe1′	7.646 (3)	Fe1–N4	1.956 (6)
Fe1–N1	1.975 (8)	Fe1–N5	1.943 (6)
Fe1–N2	1.961 (7)	Fe1–N6	1.964 (8)
Fe1–N3	1.966 (7)		

(b) Bond Angles (deg)

N1–Fe1–N2	81.5 (3)	N3–Fe1–N5	94.2 (3)
N1–Fe1–N3	94.1 (3)	N4–Fe1–N5	174.4 (2)
N2–Fe1–N3	174.6 (2)	N1–Fe1–N6	176.0 (3)
N1–Fe1–N4	87.7 (3)	N2–Fe1–N6	96.1 (3)
N2–Fe1–N4	95.6 (3)	N3–Fe1–N6	88.5 (3)
N3–Fe1–N4	81.1 (3)	N4–Fe1–N6	95.7 (3)
N1–Fe1–N5	95.7 (3)	N5–Fe1–N6	81.1 (3)
N2–Fe1–N5	89.3 (3)		

(c) Dihedral Angles (deg)[a]

bpy1,2–bpy5′,6′	32.4	bpy5,6–bpy1′,2′	32.4
bpy3,4–bpy3′,4′	40.3		

[a] The notation describes the atoms in a symmetry-unique half of each ligand that contains the numbered nitrogen atoms.

In the final difference Fourier synthesis, the maximum electron density of 1.49 e $Å^{-3}$ was located at the origin; the minimum was −1.11 e $Å^{-3}$. Analysis of variance as a function of Bragg angle, magnitude of F_o, reflection indices, etc., showed no significant trends.

Table II contains a list of atomic positional parameters and equivalent isotropic thermal parameters, while Table III contains a list of selected interatomic distances and angles for I. Available as supplementary material are lists of anisotropic thermal parameters for non-hydrogen atoms, anion distances and angles, and observed and calculated structure factors.

Results

Structure of I. The structure of the triply bridged dinuclear cationic unit of I is shown in Figure 1. The figure clearly shows how the complex achieves the metal to ligand ratio of 2:3, with the nitrogen atoms of the binucleating ligands coordinated in a pseudooctahedral fashion about each of the iron(II) atoms. The bridging dimethylene group on each ligand constrains the distance between the two bipyridyl units. The cation exhibits crystallographically required 2 (C_2) symmetry, although previous studies have shown that this cation can satisfy crystallographically imposed 32 (D_3) symmetry.[8] Although in this salt the cation is only required to have 2 symmetry, it still exhibits approximate 32 symmetry, with the noncrystallographic 3-fold axis passing through the two iron(II) atoms. Crystallographic 32 symmetry would demand that the "inner" set of Fe–N bonds (to N1, N3, and N5) would be equal in length; the "outer set" of Fe–N bond lengths would be identical as well. In I, the "inner" Fe–N distances contain

(8) Crystals of the ClO_4^- and PF_6^- salts of I have been prepared and studied by X-ray diffraction in this laboratory. Both compounds crystallized in $P\bar{3}1c$, and solution of the structures confirmed the nature of the dinuclear cation (which possessed the crystallographically required 32 symmetry in both cases). Severe disorder involving the counteranions and occluded solvent molecules ($DMSO/H_2O$) was encountered in both cases, and all attempts to model the positions of the lighter atoms of these disordered entities failed.

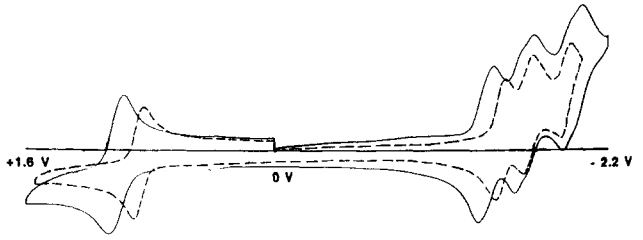

Figure 2. Cyclic voltammogram of I (—) and II (--) in CH_3CN/0.1 M (TBA)PF_6 on a glassy-carbon electrode (potentials vs SCE).

Table IV. Electrochemical Data

compd	couple	$E_{1/2}$(DPV), V	$E_{1/2}$(OSWV), V	$\Delta E_{1/2}$(OSWV), V
I	3+,3+/3+,2+	+1.005	+0.997	70
	3+,2+/2+,2+	+1.076	+1.067	
	2+,2+/2+,1+	-1.353	-1.353	75
	2+,1+/1+,1+	-1.417	-1.428	
	1+,1+/1+,0	-1.588	-1.600	84
	1+,0/0,0	-1.675	-1.684	
	0,0/0,1-	-1.912	-1.912	85
	0,1-/1-,1-	-1.995	-1.997	
II	3+/2+	+0.912	+0.896	
	2+/1+	-1.460	-1.464	
	1+/0	-1.652	-1.652	
	0/1-	-1.898	-1.898	

one distance (Fe1–N5) that is significantly different from the other two, while the "outer" Fe–N distances are equal within experimental error. The Fe(II) atoms are separated by 7.646 (3) Å in the solid state.

Cyclic Voltammetry. Cyclic voltammograms (CV's) of I and II are shown in Figure 2. For the mononuclear complex, II, there are three reversible ligand-based reduction waves in the potential region 0.0 to -2.1 V and one metal-based oxidation wave in the region 0.0 to +1.6 V (hereafter, for simplicity, each of the redox processes will be referred to in terms of the formal oxidation state of the metal even though reductions beyond the 2+ state are ligand-based). Comparison of the data in Figure 2 reveals two important differences in the voltammograms of the two complexes. First, the waves for the dinuclear Fe complex, I, are, in general, shifted relative to those for the mononuclear Fe complex, II. Second, the voltammetric waves for the dinuclear complex are broadened relative to those for the mononuclear complex, and, in fact, in the cases of the nominal 1+/0 and 0/1- processes the waves are partially resolved into two peaks. This type of voltammetric behavior is typical of systems having two interacting redox sites. The unusual feature of this system, however, is that the saturated nature of the CH_2–CH_2 bridges in the ligand of I precludes through-bond charge delocalization. It thus follows that the site–site interaction reflected in the voltammetric data must result from a through-space electrostatic interaction.

Since the individual redox processes for the dinuclear complex are poorly resolved in the CV experiment, individual $E_{1/2}$ potentials cannot be easily or accurately extracted from this data. In this type of situation other voltammetric techniques such as differential-pulse voltammetry and/or square-wave voltammetry provide better means to obtain the desired potential information. Therefore, a consideration of relative potential shifts for corresponding redox processes in I and II will be given in the context of these experiments.

Differential-Pulse Voltammetry (DPV). Richardson and Taube[9] have described a DPV technique to determine the difference in the $E_{1/2}$'s for unresolved waves in reversible systems. This technique involves the use of a working curve to convert the peak width at half-height of the DPV peak into $\Delta E_{1/2}$ between the two closely spaced redox processes. DPV was performed on the dinuclear Fe complex I and the mononuclear Fe complex II and also on the Ru complex III for comparison.

The peak width at half-height for a single, reversible one-electron-redox process under the experimental conditions employed here is predicted from the equation of Perry and Osteryoung[10] to be 90.9 mV. The experimental widths of the peaks at half-height ($W_{1/2}$) measured for II were 91 ± 10 mV. The $W_{1/2}$'s for I, on the other hand, ranged from 124 to 167 mV. The individual $E_{1/2}$'s calculated by the method described above are given in Table IV. As with complex I the Ru complex III also undergoes two one-electron-redox changes for each peak; however, the $W_{1/2}$'s of the DPV peaks for III were 91 ± 10 mV, indicating that there is no observable interaction between the Ru centers in this complex.

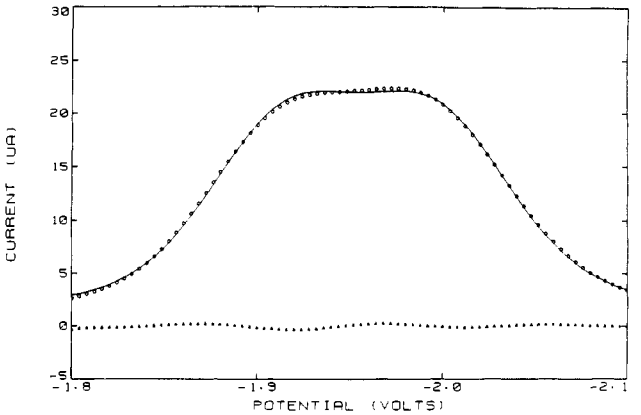

Figure 3. OSWV voltammogram for the 0,0/0,1- and 0,1-/1-,1- couples in I: (○) experimental current; (—) best-fitting theoretical curve, (▽) residuals (experimental–theoretical fit). Conditions: step height 4 mV; square-wave amplitude 25 mV; square-wave frequency 15 Hz; $(1 - R) = 2 \times 10^{-4}$.

Osteryoung Square-Wave Voltammetry (OSWV). OSWV was carried out on the dinuclear Fe complex, the mononuclear Fe complex, and the Ru complex. The data from the OSWV experiment for complex I were analyzed according to a nonlinear least-squares procedure[11] implemented by the COOL algorithm.[12] This is a method equivalent to the method of maximum likelihood in which the correlation of the experimental current with a computed theoretical current is maximized by finding the values of rate parameters that yield a value for the correlation coefficient (R) nearest unity. For the data discussed here values of $1 - R$ are in the range ≤0.002. The modified simplex algorithm is used for the search. Values of the theoretical current are calculated by numerical integration of the equation describing the model. The general procedure has been discussed for square-wave voltammetry by O'Dea, et al.;[13] detailed computations for the EE and ECE cases will appear elsewhere.[14]

Figure 3 shows the experimental OSWV data, the numerical fit, and the residual for the 0,0/0,1- and 0,1-/1-,1- couples in I. The $E_{1/2}$'s thus obtained are also listed in Table IV. Under the conditions employed, the width of a peak for a single reversible redox process should be 98.8 mV.[15] The width of the peaks for the mononuclear Fe complex and the Ru complex was 99 ± 5 mV. The major advantage of the OSWV approach over that used in the DPV procedure is that in the former case the data are a fit for the entire voltammetric peak whereas the DPV method basically employs two points. In any event, for these well-behaved and simple chemical systems, both methods produce very similar results.

Discussion

From the structural data for I, the iron atoms are separated by 7.646 (3) Å. Employing a simple electrostatic model which assumes that the changes in oxidation state of the dinuclear complex are localized at the metal centers, it is possible to calculate an electrostatic difference in the redox potential for the halves

(9) Richardson, D. E.; Taube, H. *Inorg. Chem.* **1981**, *20*, 1278.

(10) Perry, E. P.; Osteryoung, R. A. *Anal. Chem.* **1965**, *37*, 1634.
(11) O'Dea, J.; Osteryoung, J.; Lane, T. *J. Phys. Chem.* **1986**, *90*, 2761.
(12) O'Dea, J., SUNY/Buffalo.
(13) O'Dea, J.; Osteryoung, J.; Osteryoung, R. *Anal. Chem.* **1981**, *53*, 695.
(14) O'Dea, J.; Osteryoung, J., unpublished work, SUNY/Buffalo.
(15) Ramaley, L.; Krause, M. S. *Anal. Chem.* **1969**, *41*, 1362.

of the complex.[16] Obviously, for the oxidation state changes that are ligand-based, such a model is, in a quantitative sense, inappropriate. However, for the metal-centered 3+/2+ process, the model is a reasonable first-order approximation. Using this approach, assuming a continuous dielectric with a dielectric constant equal to that of acetonitrile, one obtains a $\Delta E_{1/2}$ value of 49 mV. Alternatively, if the dielectric constant for pyridine is employed in the calculation, a $\Delta E_{1/2}$ value of 154 mV is obtained. The experimental $\Delta E_{1/2}$ values obtained from DPV and OSWV data for the 2+,2+/3+,2+ and 3+,2+/3+,3+ processes (Table IV) lie between the two above calculated values. Consideration of Figure 1 reveals that in the space between the two metal centers in I, the acetonitrile solvent is excluded by the presence of the ligands. The dielectric medium in this region is thus more "pyridine-like". It is reasonable then that the measured $\Delta E_{1/2}$ should lie somewhere between the two calculated values.

As stated above, when the redox change is ligand-based, as it is for all but the 2+/3+ process, the quantitative aspects of the above model break down because the positions of the interacting charges are not precisely known; nonetheless, some distance limits can be established for the location of the charges. Qualitatively, for the ligand-based processes, the simple electrostatic model predicts $\Delta E_{1/2}$ values similar to those calculated for the metal-based processes. Examination of the data in Table I indicates that again the prediction of the model is consistent with experiment in that the $\Delta E_{1/2}$ values for the ligand-based processes are of the same order of magnitude as observed for the metal-based oxidations.

The metal–metal distance in complex III can be approximated from molecular models to be about twice that in I. All other things being equal, one would thus expect an electrostatic factor in this complex of roughly half that observed in I; however, no splitting is observed. A single reversible wave is obtained in the CV for III having an $E_{1/2}$ value that is identical with that of the previously studied mononuclear analogue, $Ru(Bpy)_2(Me_2bpy)^{2+}$.[7] In addition to simple distance differences, one must consider the fact that the dielectric medium between the two linked tris(bipyridine) complexes in I and III is almost certainly quite different. On the basis of examination of molecular models, the single linkage in III should not significantly exclude solvent and electrolyte ions from the region between the two centers the way the triple linkage in I does. Thus, considering both the increased distance and the expected increase in local dielectric constant, it is reasonable that in such a complex as III, that the electrostatic interaction should be vanishingly small.

Electrostatic considerations can be extended to a comparison of the voltammetric data of I and II as well. In the absence of any site–site interaction, previously reported data on mononuclear metal complexes indicate that the redox potentials of I and II should be, within experimental error identical;[7,17] the reason for this is that the methyl substituents in the ligands of II are electronically equivalent to the methylene substituent of the bridging ligand in I. Consequently, any differences in the redox potentials of the two complexes must arise from site–site interactions. In other words the presence of the second site in the dinuclear complex I introduces an additional electrostatic work term that will shift the redox potential of the dinuclear complex relative to the analogous process in the mononuclear complex. The first oxidation of the dinuclear complex (2+,2+/2+,3+) is shifted significantly in the positive direction relative to the mononuclear complex 2+/3+ process. The presence of the positively charged second site in the dinuclear complex thus increases the work necessary to remove the first electron from the dinuclear complex relative to the same process in the mononuclear species. The first reduction process for I is also shifted to more positive potentials relative to that of the mononuclear complex. Again, this is consistent with charge effects; in the first reduction, the charge as well as the formal oxidation state of the complex is reduced, thus making it more favorable to reduce the dinuclear complex over the mononuclear complex. The first peak for the second pair of reductions of the dinuclear complex (1+,1+/1+,0) is also more positive than the mononuclear complex, again, based on the same reasoning. However, the second reduction in this pair (1+,0/0,0) and the first reduction of the next pair (0,0/1−,0) should experience little or no electrostatic difference from the mononuclear complex since in each case both complexes have the same overall charge. Examination of the data in Table IV reveals that, as predicted, the 1+/0 and 0/1− couples for the mononuclear complex occur at very nearly the same potentials (vide infra) as the 1+,0/0,0 and 0,0/1−,0 couples, respectively, for the dinuclear complex. The second reduction of the dinuclear complex in this last pair (1−,0/1−,1−) occurs at a significantly more negative potential than the 0/1− couple in the mononuclear complex, again for analogous reasons; the second reduction "feels" the presence of the negative charge and thus becomes more difficult, by 100 mV, to effect.

The 1+/0 and 0/1− couples for the mononuclear complex and the 1+,0/0,0 and 0,0/1−,0 couples for the dinuclear complex, while very close, do not occur at exactly the same potentials (differences of 21 and 14 mV, respectively, based on the OSWV data). These small differences may be accounted for by the facts that the dielectric media for I and II are not identical (by nature of the presence of the other half of the dinuclear unit in II) and that these redox processes are not localized at the metal centers, as assumed by the model but, rather, are ligand-localized.

While this electrostatic model lacks the details to quantitatively predict the voltammetric results, all of the qualitative results are totally consistent with the model. In addition to the electrochemical results, it is possible to rationalize, at least in part, the synthesis of the dinuclear complex on the basis of electrostatic arguments as well. Entropically, one would not predict that a single, dinuclear product would result from the synthesis employed to prepare I. In fact, when the Fe^{2+} and the bridging ligand are mixed, a variety of products are formed initially including some insoluble (presumed polymeric) material. Following the course of the reaction by TLC, however, one finds that after ~15 min of reflux the thermodynamically favored dinuclear complex has become the only product. For comparison, an analogous reaction was conducted employing a similar type of bridging ligand to that present in I but one having five, rather than two, methylene units in the bridge. Initially, when the five-carbon-bridged ligand and Fe^{2+} are mixed, the product distribution (by TLC) is quite similar to that obtained initially for the two-carbon-bridged ligand in I, but upon reflux, the five-carbon analogue remains as a complex mixture of products (even after several hours of heating). Electrostatic arguments can be used to explain these results in the following way. If one considers all of the possible product distributions, assuming each iron is bound to three bipyridines, in every arrangement possible other than the structure of I, each iron is bound to at least two other iron complexes and in most cases is bound to three. The iron–iron electrostatic repulsion is thus minimized in the structure in Figure 1. For the five-carbon-bridged binucleating analogue the iron–iron distances are much larger and the electrostatic repulsion terms are smaller (calculated to be significantly less than kT); thus, entropic considerations prevail.

Finally, the type of chemistry reported above is not unique to Fe^{2+}. Dinuclear complexes of Co^{2+}, Mn^{2+}, and Ni^{2+} have also been synthesized by basically the same route as that used to prepare I and with basically the same results. All of these dinuclear complexes show the same qualitative type of redox behavior as the Fe complex; however, the electrochemistry is typically not as simple. Many of the redox processes for these additional complexes are chemically irreversible (in much the same way as the redox processes for the respective mononuclear species are irreversible). In cases where reversible processes exist, for example the Co 2+/1+ couple, the results closely parallel those obtained for the iron case. If, as our results indicate, the interactions in the complexes are electrostatic in nature, they should be more or less independent of the metals involved.

(16) By use of the simple electrostatic equation $-q^2/4\pi\epsilon r = \Delta E_{1/2}$.
(17) Schmehl, R. H.; Auerbach, R. A.; Wacholtz, W. F.; Elliott, C. M.; Freitag, R. A.; Merkert, J. W. *Inorg. Chem.* **1986**, *25*, 2440.

Summary

The triply bridged complex I constitutes an unusual example of a compound having an enforced geometry that allows for the demonstration of a significant and experimentally measurable degree of pure electrostatic interaction. Typically, because of the requirement of saturated linkages to prevent through-bond charge delocalization, such interactions are not observable. Both the synthesis and electrochemistry of this dinuclear complex are semiquantitatively explainable in terms of simple electrostatics. Finally, the behavior of the Fe complex is not unique; the general features reported here appear to extend to other isostructural complexes, as well.

Acknowledgment. We thank the National Science Foundation (Grant No. CHE 8516904) for generous support of this work. The Nicolet R3m diffractometer and computing system were purchased with funds provided by the National Science Foundation (Grant No. CHE 8103011). We also thank J. Osteryoung and J. O'Dea for analyzing the OSWV data.

Registry No. I^{6+}, 117251-64-6; I^{5+}, 117251-65-7; I^{3+}, 117251-66-8; I^{2+}, 117251-67-9; I^{+}, 117251-68-0; I, 117251-69-1; I^{-}, 117251-70-4; I^{2-}, 117251-71-5; $I(CF_3SO_3)_4$, 117251-61-3; $I(ClO_4)_4$, 117251-58-8; $I(PF_6)_4$, 117251-59-9; II^{3+}, 34032-03-6; II^{+}, 71619-84-6; II, 20515-12-2; II^{-}, 71619-85-7; $II(PF_6)_2$, 85185-57-5; III, 117251-63-5; $Ru(bpy)_2Cl_2$, 15746-57-3.

Supplementary Material Available: Tables of crystallographic details, bond lengths, bond angles, anisotropic thermal parameters, and hydrogen atom parameters for I (11 pages); a table of observed and calculated structure factors (34 pages). Ordering information is given on any current masthead page.

Notes

Contribution from the Departments of Inorganic and Physical Chemistry, University of Melbourne, Parkville, Victoria 3052, Australia

Electronic Spectra of the Solvated Cations of Chromium(III) and Manganese(II) in Anhydrous Hydrogen Fluoride

Colin G. Barraclough,* Russell W. Cockman, Thomas A. O'Donnell,* and Margaret J. Snare

Received January 5, 1988

Previous work from this laboratory has shown that whereas transition-metal difluorides and trifluorides have very low solubilities in anhydrous hydrogen fluoride (AHF), solutions of transition-metal cations in AHF can be prepared by reaction of a transition metal or its fluoride with AHF, the acidity of which has been enhanced deliberately by addition of an appropriate Lewis acid such as BF_3, AsF_5, or SbF_5. UV-visible and Raman spectra of many such solutions have been reported.[1-4]

The previous electronic spectra were interpreted in crystal field terms, with the perturbing field assumed to be due to coordinated HF molecules. The present work extends the range of ions to include Cr^{3+} and Mn^{2+}. ESR spectra of these ions in AHF have also been observed.

Experimental Procedures

Vacuum Manipulation. Volatile fluorides were transferred individually in a stainless-steel vacuum system, based on stainless-steel Swagelok unions and Whitey valves (SS-1KS4), to Kel-F reaction tubes fitted with Kel-F valves for preparation of solutions for spectroscopy. The passivating metal fluoride layer is dissolved if HF and a Lewis acid are in the metal section of the vacuum system simultaneously. However Kel-F is resistant to HF solutions of Lewis acids. High pressures of volatile compounds were measured with Bourdon gauges and pressures in the millitorr range with a Varian 801 thermocouple gauge.

Reagents. AHF. Commercially available HF (Matheson, 99.8%) was purified by four trap-to-trap distillations in a well-conditioned Kel-F apparatus, using $CaCl_2$-H_2O-dry ice as the coolant for condensation at -45 °C and discarding "heads and tails". Purity was checked by measurement of electrical conductance, the value typically being 1×10^{-4} Ω^{-1} cm^{-1} at 0 °C.

F_2 and AsF_5. F_2 (Matheson) and AsF_5 (Ozark-Mahoning) were used as received.

SbF_5. The purification procedure previously reported[5] was followed, with collection of the fraction boiling in the range 143-145 °C. Since SbF_5 was effectively involatile at the vacuum line pressures used during this work, the reagent was manipulated in the form of solutions in AHF, typically approximately 5 M.

Metals. Mn (Koch Light, 99.5%) and Cr (Koch Light 99.4%) were used as massive metal, rather than powders, in order to minimize contamination by surface oxides. Surface oxide was removed as reported earlier.[4]

Preparation of Solutions. $(NH_4)_3CrF_6$. The solid fluorochromate was prepared according to the method of Sturm.[6] Solutions of the solid in "neutral" AHF were not entirely stable, precipitation of CrF_3 occurring on standing. Stable green solutions were obtained by using a large excess of fluoride, typically 5 M in NH_4F.

$Mn(AsF_6)_2$. In a typical run, 0.55 g of cleaned metallic Mn was weighed into a Kel-F tube. After evacuation, AHF (20 cm^3) was distilled in and excess AsF_5 (measured by *PVT* relationships) was added at -196 °C. The contents were allowed to warm to ambient temperature, and initiation of reaction was indicated by the evolution of a gas not condensable at -196 °C, hydrogen. After the mixture was allowed to stand overnight, the metal had dissolved, forming a clear colorless solution, which was solidified by cooling, and the quantity of H_2 formed was measured. This was never found to be as required by eq i because some of the excess AsF_5 acted as an oxidant according to eq ii. The presence

$$Mn + 2HF + 2AsF_5 \rightarrow Mn_{solv}^{2+} + H_2 + 2AsF_6^- \quad \text{(i)}$$

$$Mn + 3AsF_5 \xrightarrow{HF} Mn_{solv}^{2+} + AsF_3 + 2AsF_6^- \quad \text{(ii)}$$

of the AsF_3 impurity was found to have no detrimental effect on the subsequent spectroscopic studies reported here.

For analysis, a known volume of the solution of Mn^{2+} in AHF was dissolved in water and oxidized to MnO_4^-, which was determined spectrophotometrically at 525 nm.

$Cr(SbF_6)_3$. Massive crystalline chromium (0.04 g) was weighed into a Kel-F tube, which was evacuated. A 6 M solution of SbF_5 in AHF (5 cm^3) was introduced into the evacuated tube, and reaction was allowed to occur at ambient temperature. After several hours the metal had dissolved, leaving a pale green-blue solution, which was shown by UV-visible spectroscopy[2] to contain Cr_{solv}^{2+}. As noted above the stoichiometric quantity of hydrogen expected from eq iii was not observed, indicating that some of the SbF_5 had been reduced during the reaction (see eq ii).

$$Cr + 2HF + 2SbF_5 \xrightarrow{HF} Cr_{solv}^{2+} + H_2 + 2SbF_6^- \quad \text{(iii)}$$

Caution! For the subsequent step it is imperative that all of the liberated hydrogen is removed by repeatedly freezing the solution and pumping off H_2. Fluorine, in a small excess over that required to convert Cr(II) to Cr(III) by eq iv, was added at -196 °C, and the reaction was

$$2Cr_{solv}^{2+} + F_2 + 2SbF_5 \rightarrow 2Cr_{solv}^{3+} + 2SbF_6^- \quad \text{(iv)}$$

allowed to proceed as the solution warmed to ambient temperature. If

(1) Barraclough, C. G.; Cockman, R. W.; O'Donnell, T. A. *Inorg. Chem.* **1977**, *16*, 673.
(2) Baluka, M.; Edelstein, N.; O'Donnell, T. A. *Inorg. Chem.* **1981**, *20*, 3279.
(3) Barraclough, C. G.; Cockman, R. W.; O'Donnell, T. A. *Inorg. Nucl. Chem. Lett.* **1981**, *17*, 83.
(4) Barraclough, C. G.; Cockman, R. W.; O'Donnell, T. A.; Schofield, W. S. J. *Inorg. Chem.* **1982**, *21*, 2519.
(5) Gillespie, R. J.; Peel, T. E. *J. Am. Chem. Soc.* **1973**, *95*, 5173.
(6) Sturm, B. J. *Inorg. Chem.* **1962**, *1*, 665.

0020-1669/88/1327-4504$01.50/0